Biomaterials 272 (2021) 120780

Contents lists available at ScienceDirect

Biomaterials

journal homepage: www.elsevier.com/locate/biomaterials

PEGylation of poly(amine-co-ester) polyplexes for tunable gene delivery

Molly K. Grun [a], Alexandra Suberi [b], Kwangsoo Shin [b], Teresa Lee [b], Victoria Gomerdinger [a], Zoe M. Moscato [b], Alexandra S. Piotrowski-Daspit [b,**], W. Mark Saltzman [a,b,c,d,*]

[a] Department of Chemical & Environmental Engineering, Yale University, New Haven, CT, 06511, USA
[b] Department of Biomedical Engineering, Yale University, New Haven, CT, 06511, USA
[c] Department of Cellular & Molecular Physiology, Yale University, New Haven, CT, 06511, USA
[d] Department of Dermatology, Yale School of Medicine, New Haven, CT, 06510, USA

ARTICLE INFO

Keywords:
Gene delivery
Polymeric vehicle
Polyplex
Poly(ethylene glycol)
Biodegradable
Biocompatible

ABSTRACT

There is growing interest in PEGylation of cationic polymeric vehicles for gene delivery in order to improve vehicle stability and reduce toxicity, but little is known about the effects of PEG coatings on transfection. We used a polymer from the poly(amine-co-ester) (PACE) family blended with PEG-conjugated PACE at different ratios in order to explore the effects of polyplex PEGylation on the transfection efficiency of plasmid DNA, mRNA, and siRNA *in vitro* and mRNA *in vivo*. We discovered that concentrations of PACE-PEG as low as 0.25% by weight improved polyplex stability but also inhibited transfection *in vitro*. *In vivo*, the effect of PACE-PEG incorporation on mRNA transfection varied by delivery route; the addition of PACE-PEG improved local delivery to the lung, but PEGylation had little effect on intravenous systemic delivery. By both delivery routes, transfection was inhibited at concentrations higher than 5 wt% PACE-PEG. These results demonstrate that excess PEGylation can be detrimental to vehicle function, and suggest that PEGylation of cationic vehicles must be optimized by PEG content, cargo type, and delivery route.

1. Introduction

Cationic polymer vehicles have been widely studied as a promising alternative to viral vectors for gene therapy because of their non-immunogenicity, scalability, and versatile chemistry, which can be tuned to deliver diverse nucleic acids such as DNA, mRNA and siRNA [1,2]. Positively charged polymers can efficiently condense nucleic acids and mediate cellular uptake through interactions with the negatively charged cell membrane [3,4]. Among cationic polymers, biodegradable polymers—such as polyesters, polycarbonates, and polyurethanes—show promise as gene delivery vectors due to their improved biocompatibility [5]. In recent years, researchers have explored a number of approaches to improve vehicle stability and gene delivery efficiency while minimizing cytotoxic effects of biodegradable polymers. These strategies include screening monomer combinations [6,7]; conjugating end-capping groups to the polymer backbone [7,8]; incorporating degradable bonds such as disulfides [5]; and adding surface coatings such as targeting ligands or poly(ethylene glycol) (PEG) [1,9].

PEG coatings have become an integral part of polymer vehicle design due to the numerous beneficial effects of PEG. PEGylation has been shown to improve vehicle stability [10,11], extend *in vivo* half-life [12,13], and reduce toxicity [2,14,15]. PEG coatings can also improve nanoparticle (NP) penetration through mucus [16,17]. However, several limitations of PEG-coated NPs have also been reported, such as decreased transfection efficiency [18], decreased cellular uptake [19,20], and the establishment of anti-PEG immunity after repeated doses *in vivo* [21,22]. There are many potential benefits to PEGylating cationic polymer NPs and polyplexes, such as decreased toxicity, improved stability, and enhanced tissue penetration; however, the effect of PEGylation on nucleic acid transfection efficiency remains unclear. *In vitro*, some researchers have reported unchanged or improved transfection

Abbreviations: BSA, bovine serum albumin; DES, diethyl sebacate; SA, sebacic acid; MDEA, methyl diethanolamine; PDL, pentadecanolide; DLS, dynamic light scattering; GPC, gel permeation chromatography; MW, molecular weight; NMR, nuclear magnetic resonance; PDI, polydispersity index; NP, nanoparticle; PACE, poly(amine-co-ester); PBAE, poly(β-amino ester); PEG, poly(ethylene glycol); PEI, polyethyleneimine; TEM, transmission electron microscopy; FBS, fetal bovine serum; IT, intratracheal; IV, intravenous.

* Corresponding author. Malone Engineering Center Room 413, 55 Prospect Street, New Haven, CT, 06511, New Haven, USA.
** Corresponding author. Malone Engineering Center Room 401E, 55 Prospect Street, New Haven, CT, 06511, New Haven, USA.
E-mail addresses: alexandra.piotrowski-daspit@yale.edu (A.S. Piotrowski-Daspit), mark.saltzman@yale.edu (W.M. Saltzman).

https://doi.org/10.1016/j.biomaterials.2021.120780
Received 4 December 2020; Received in revised form 19 March 2021; Accepted 20 March 2021
Available online 24 March 2021

with PEG coatings [23], while others have reported that transfection is inhibited [10,20]. Several studies have suggested that the transfection efficiency of PEG-conjugated polymers can be optimized by adjusting parameters such as PEG molecular weight (MW) and polymer to nucleic acid N:P ratio [11,24–27]. Furthermore, *in vitro* screens frequently correlate poorly with *in vivo* results. For example, Mastorakos et al. found that PEG decreased transfection efficiency of poly(β-amino ester) (PBAE) polyplexes *in vitro* but improved transfection via inhaled delivery in mice [28]. Williford et al. grafted PEG to polyethyleneimine (PEI) to varying degrees and observed that transfection was inhibited at lower PEG densities *in vivo* (IV delivery in mice) as compared to *in vitro* experiments [29]. Apart from optimizing PEG coverage, many additional strategies have been investigated to overcome the "PEG dilemma"; these approaches include attaching targeting ligands to the vehicle surface and developing cleavable PEG coatings that detach in response to specific stimuli such as temperature, pH, enzymes, or reductive conditions [18,30]. Overall, these reports suggest that more comprehensive studies—investigating cargo type, *in vivo* administration route, and PEG content—are needed to understand and optimize the advantages of PEGylation for gene therapy.

We have recently described a family of cationic polymers, poly (amine-co-esters) (PACEs), that can effectively deliver a variety of nucleic acids *in vitro* and *in vivo* [2,6]. PACE polymers are biodegradable and highly customizable; by varying component monomers and lactone content, we have created a library of materials with tunable characteristics, such as hydrophobicity, thermal properties, MW, toxicity, and transfection efficiency. When synthesized with lower lactone content (10–20%), PACE polymers can be used to formulate polyplexes with negatively charged nucleic acids. Synthesis of this versatile class of polymers can also be modified to incorporate PEG groups, producing PACE-PEG block copolymers. Here, we have comprehensively investigated the effects of PEG content and nucleic acid cargo type on the efficacy of gene delivery. We formulated PACE polyplexes with a range of PEG content by blending PACE with PEG-conjugated PACE (PACE-PEG) in order to examine the effect of PEGylation on the transfection efficiency, stability, and toxicity of PACE polyplexes for the delivery of different nucleic acids *in vitro* and *in vivo* both locally and systemically. PEGylation offers both advantages and disadvantages, and we explore the intersection of these effects and how they can differ *in vitro* and *in vivo*. We describe an approach to produce versatile, biocompatible, and stable polyplexes encapsulating a wide size range of nucleic acids. This study highlights the importance of testing and optimizing PEG coverage of polymeric vehicles for gene therapy applications.

2. Materials and methods

2.1. Materials and reagents

PEG, 15-pentadecanolide (PDL), N-methyl diethanolamine (MDEA), sebacic acid (SA), diethyl sebacate (DES), diphenyl ether, Novozym 435 catalyst, bovine serum albumin (BSA), Roche cOmplete EDTA-free Protease Inhibitor Cocktail, and Immobilon-FL PVDF membranes were purchased from MilliporeSigma (Saint Louis, MO, USA). pcDNA3-EGFP plasmid was obtained from Addgene (Watertown, MA, USA). CleanCap EGFP mRNA and CleanCap FLuc mRNA were purchased from TriLink Biotechnologies (San Diego, CA, USA). siRNA against nectin-1 (GGUUAAAAGGUGAGGCAGA) was synthesized by Horizon Discovery (Waterbeach, United Kingdom). For cell culture, HeLa cells and Eagle's Modified Essential Medium (EMEM) were purchased from ATCC (Manassas, VA, USA), and fetal bovine serum (FBS) was purchased from R&D Systems (Minneapolis, MN, USA). Lipofectamine products, TrypLE Express Enzyme, MOPS SDS running buffer, 10% NuPAGE Bis-Tris Gel, nectin-1 monoclonal antibody (clone CK8), HRP-conjugated goat anti-mouse IgG (H + L) secondary antibody, and the Pierce BCA Protein Assay were obtained from Thermo Fisher Scientific (Waltham, MA, USA). PE anti-human CD111 (nectin-1) antibody was purchased from BioLegend (San Diego, CA, USA). β-actin monoclonal antibody was purchased from Proteintech Group (Rosemont, IL, USA). Clarity Western ECL substrate was purchased from Bio-Rad Laboratories (Hercules, CA, USA). CellTiter-Glo, Glo Lysis Buffer, and the Bright-Glo Luciferase Assay System were purchased from Promega (Madison, WI, USA). Precellys hard tissue lysing tubes were obtained from Bertin Instruments (Montigny-le-Bretonneux, France). RediJect D-Luciferin Substrate was purchased from PerkinElmer (Waltham, MA, USA).

2.2. Polymer synthesis, purification, and characterization

PACE polymers were synthesized as described previously, with some modifications [2,6]. Briefly, the monomers (PDL, MDEA, and SA) were dissolved in diphenyl ether solvent with a lipase-based Novozym 435 catalyst. In the first stage, monomers were oligomerized at 1 atm under argon for 18–20 h at 90 °C. This was followed by 48–72 h of polymerization at 90 °C under vacuum (2 mmHg; Figure S1). Polymers were then purified following previously described methods [2]. For the synthesis of PACE-PEG, 5000 molecular weight (MW) PEG was added as an additional monomer and DES was substituted for SA. The synthesis was otherwise identical. 10 mol% PDL content was used for all polymers in this study. To determine their composition, polymers were dissolved in deuterated chloroform and analyzed via proton nuclear magnetic resonance (1H NMR, Agilent DD2 400 MHz NMR Spectrometer). MW was determined by GPC using the Ultimate 3000 UHPLC system (Thermo Fisher Scientific).

2.3. Polyplex formulation and characterization

All PACE polyplexes were formed at a weight ratio of 100:1 polymer to nucleic acid. Polymers were dissolved 100 mg/mL in DMSO overnight at 37 °C while shaking. To make blends of PACE and PACE-PEG, the dissolved PACE and PACE-PEG polymers were combined at the indicated weight percentage. Intermediate dilutions were made as necessary. Here, we refer to the PACE-PEG content of polyplex formulations, but the theoretical PEG content can be calculated (Table S1). For characterization and *in vitro* experiments, nucleic acids were diluted into sodium acetate buffer (25 mM, pH 6) to a final concentration of 20 μg/mL (pDNA and mRNA) or 1 μM (siRNA). Polymers were similarly diluted into sodium acetate buffer (25 mM, pH 6) to a final concentration of 2 mg/mL (pDNA and mRNA) or 1.33 mg/mL (siRNA) and vortexed for 15 s. The polymer solution was then added to the nucleic acid solution at 1:1 vol ratio and vortexed for an additional 25 s. The polyplexes were incubated at room temperature for 10 min before use (adding directly to cell culture medium). Polyplex size and zeta potential were measured by dynamic light scattering (DLS, Zetasizer Pro, Malvern Analytical). Size and morphology were also confirmed by transmission electron microscopy (TEM, FEI Tecnai Osiris 200 kV) using a tungsten stain for visualization.

2.4. Polyplex stability assessment

To assess their stability over time, polyplexes were formulated in sodium acetate buffer (25 mM, pH 6) to a final concentration of 2 mg/mL and placed in a 37 °C incubator shaking at 200 rpm. For stability assessments in serum, 10% FBS was added to the sodium acetate buffer after polyplexes were formulated. Polyplex size was measured by DLS (Zetasizer Pro, Malvern Analytical) at each time point (0 h, 0.5 h, 1 h, 2 h, 4 h, 8 h, 24 h, 48 h, 72 h) or until the PDI = 1 or multiple peaks were observed. Polyplexes were diluted to 40 μg/mL in deionized water prior to measurement.

2.5. In vitro toxicity studies

HeLa cells were grown in EMEM with 10% FBS and 50 μg/mL gentamicin in a 37 °C incubator under 5% CO_2. CellTiter-Glo was used to

assess polyplex cytotoxicity *in vitro*. 24 h prior to treatment, HeLa cells were plated in 96-well tissue culture plates at a concentration of 10,000 cells per well. PACE polyplexes were delivered at varying concentrations (pDNA and mRNA: 0.313–10 μg/mL; siRNA: 6.25–200 nM). The Lipofectamine controls (Lipofectamine 3000, Lipofectamine MessengerMAX, and Lipofectamine RNAiMAX) were formulated by following the manufacturer's recommended lipid to nucleic acid ratio and delivered at the same nucleic acid concentrations. 24 h after delivery, the cell culture medium was refreshed, 100 μL of CellTiter-Glo reagent was added to each well, and plates were incubated at room temperature for 10 min. Luminescence was then measured with a plate reader using an integration time of 0.5 s per well.

2.6. In vitro transfection of pDNA, mRNA, and siRNA

HeLa cells were grown in EMEM with 10% FBS and 50 μg/mL gentamicin in a 37 °C incubator under 5% CO_2. For all transfection experiments, HeLa cells were plated at 50,000 cells per well in 24-well tissue culture plates and grown until they reached 60–80% confluency (approximately 24 h). pcDNA3-EGFP plasmid was used for plasmid DNA transfection experiments. Cells were treated for 48 h with 1 μg of plasmid per well using PACE polyplexes blended with PACE-PEG (concentrations: 0%, 0.01%, 0.025%, 0.05%, 0.1%, 0.25%, 0.5%, 1%, 2.5%) or Lipofectamine3000 according to the manufacturer's protocol as a control. For mRNA transfection experiments, cells were treated for 24 h with 1 μg of EGFP mRNA using PACE polyplexes, or Lipofectamine MessengerMAX according to the manufacturer's protocol as a control. An siRNA against nectin-1 was used for siRNA transfection experiments. Cells were treated for 72 h with 100 nM siRNA with PACE polyplexes, or 10 nM siRNA with Lipofectamine RNAiMAX according to the manufacturer's protocol as a control.

2.7. Flow cytometry, microscopy, and western blot analysis

For flow cytometry analyses, cells transfected with EGFP pDNA and mRNA were washed once with PBS, dissociated with TrypLE Express Enzyme, resuspended in FACS buffer (2% BSA in PBS), and run directly on the flow cytometer (Attune NxT). Cells treated with siRNA were dissociated with TrypLE Express Enzyme and subsequently stained with a PE anti-human CD111 (nectin-1) antibody in FACS Buffer for 30 min. Cells were then washed twice, resuspended in FACS buffer, and nectin-1 expression was quantified by flow cytometry. For microscopy analysis (Olympus LCPlanFl 20X, Olympus IX71), treated cells were washed three times with PBS and fixed in 4% paraformaldehyde in PBS. For Western blot analysis, protein extracts were prepared by lysing cells in RIPA lysis buffer (50 mM Tris-HCl [pH 7.5], 150 mM NaCl, 0.1% SDS, 1% NP40, 0.5% sodium deoxycholate, 1 mM β-glycerophosphate, 2.5 mM sodium pyrophosphate, 10 mM sodium fluoride, 1 mM sodium orthovanadate, 2.5 μM pepstatin A, 1 mM EDTA, and 1 mM EGTA) supplemented with cOmplete EDTA-free Protease Inhibitor Cocktail. Samples were run on a 10% NuPAGE Bis-Tris gel in MOPS SDS running buffer and transferred to a PVDF membrane. The membrane was blocked with 5% non-fat dry milk in tris buffered saline, and incubated with an anti-human nectin-1 monoclonal antibody (clone CK8) followed by a HRP-conjugated mouse secondary antibody. The membrane was visualized using Clarity Western ECL and imaged using a ChemiDoc imaging system (Bio-Rad). A β-actin antibody was used to probe for the loading control. Western blot quantification was performed using Image Studio Lite (LI-COR Biosciences).

2.8. In vivo mRNA delivery

All animal procedures were performed in accordance with the guidelines and policies of the Yale Animal Resource Center (YARC) and approved by the Institutional Animal Care and Use Committee (IACUC) of Yale University. Male BALB/c mice, 7–12 weeks of age, were purchased from The Jackson Laboratory (Bar Harbor, ME, USA). For *in vivo* experiments, PACE polyplexes were delivered either by intracheal instillation (IT) or intravenously (IV). Polyplexes were prepared in sodium acetate buffer (25 mM, pH 5.8) to a final concentration of 10 mg/mL polymer and 0.1 mg/mL FLuc mRNA (IT delivery) or 5 mg/mL polymer and 0.05 mg/mL FLuc mRNA (IV delivery). For IT delivery, mice were anesthetized under 3% isofluorane (Patterson Veterinary) and suspended by the incisors. The tongue was retracted with tweezers, and 50 μL of the polyplex formulations were administered to the back of the mouth. The tongue was held in the retracted position for the duration of 10 breaths while polyplexes were inhaled. For IV delivery, mice were similarly anesthetized under 3% isoflurane and then 100 μL of the polyplex formulations were delivered via retro-orbital injection. After 24 h, mice were euthanized and heart perfused with 15 mL PBS. Organs (IT: lung; IV: lung, spleen, liver, kidney) were removed, minced, and transferred to 2 mL Precellys hard tissue lysing tubes with 1 mL Glo Lysis Buffer. Organs were homogenized at 6500 rpm twice for 30 s (Precellys 24) and subsequently centrifuged at 21,000×*g* for 10 min to remove cell debris. 20 μL of tissue lysates were combined with 100 μL Bright-Glo luciferase substrate and luminescence was measured using an integration time of 10 s (Promega GloMax 20/20). The Pierce BCA Protein Assay Kit was used to measure total protein concentration following the manufacturer's instructions. For IVIS experiments, luminesence was measured 24 h after polyplex administration. 12 min prior to euthanasia, mice were injected intraperitoneally with RediJect D-Luciferin Substrate (150 mg/kg). Organs (heart, lung, liver, spleen, kidney) were removed and luminescent signal was imaged by IVIS (IVIS Spectrum, PerkinElmer).

2.9. Statistical analysis

Results were analyzed using GraphPad Prism (version 7.0a for Mac OS X). Data are presented as mean ± SD of at least three independent experiments. One- and two-way ANOVA with Tukey's multiple comparisons test were used where appropriate. Values were considered significantly different at $p < 0.05$.

3. Results and discussion

3.1. Polymer synthesis and characterization

PACE was synthesized by the enzymatic co-polymerization of PDL, MDEA, and SA as described previously [2]. Briefly, the monomers dissolved in diphenyl ether were combined with lipase catalyst and oligomerized under argon for 18–20 h. This was followed by 48–72 h of polymerization under vacuum. For PACE-PEG synthesis, DES was substituted for SA, and 5 kDa PEG was added to the synthesis (Fig. 1A). Polymer characterization, including gel permeation chromatography (GPC) analyses (Table S2) and NMR (Figure S3, Table S3) can be found in the supplementary information. Ten % PDL acid-ended PACE (referred to here as PACE) and 10% PDL PEG-conjugated PACE (PACE-PEG) were used for this study. In our experience, the synthesis of PACEs is a straightforward, two-step process that can be readily modified by the introduction of other monomers or polymer blocks such as PEG.

3.2. Polyplex formulation and characterization

We formulated PACE polyplexes to encapsulate pDNA, mRNA, or siRNA with a range of PEG content by blending PACE with PACE-PEG during assembly (Fig. 1B). PACE polyplexes were in a similar size range as measured by DLS (pDNA: 190–440 nm; mRNA: 160–360 nm; siRNA: 190–280 nm) (Fig. 2A–C). Polyplexes with 100% PACE-PEG were much smaller and had a spherical shape and smooth morphology by TEM, whereas non-PEGylated polyplexes exhibited an uneven morphology (Fig. 1C, Figure S2). Additionally, the average size tended

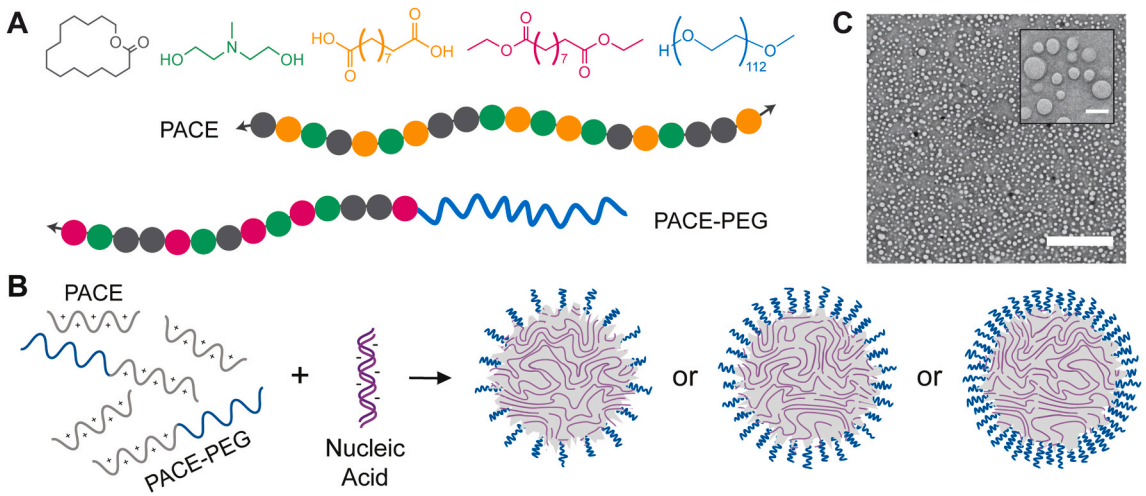

Fig. 1. Overview of PACE and PACE-PEG synthesis and polyplex formulation. **(A)** Schematic of PACE and PACE-PEG polymers with monomers pentadecanolide (PDL, grey), methyldiethanolamine (MDEA, green), sebacic acid (SA, orange), diethyl sebacate (DES, pink), and polyethylene glycol (PEG, blue). **(B)** Schematic of PACE polyplex formulation. PACE and PACE-PEG are blended and combined with nucleic acid to form polyplexes with varied PEG content. **(C)** Representative TEM image of PACE blended with 0.5% PACE-PEG loaded with siRNA (scale bar, 2 μm; inset scale bar, 200 nm). (For interpretation of the references to colour in this figure legend, the reader is referred to the Web version of this article.)

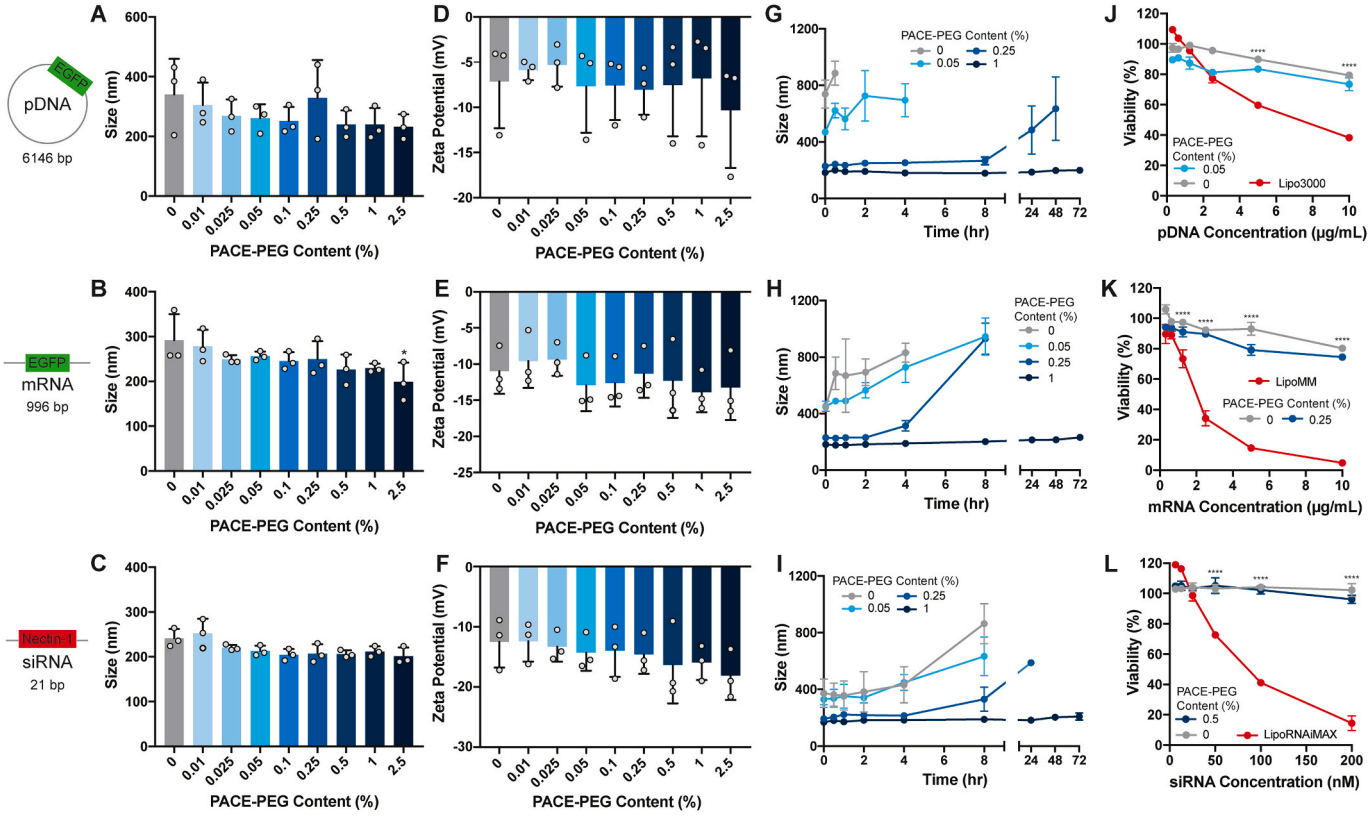

Fig. 2. PACE blended with PACE-PEG forms nanosized, stable polyplexes in the presence of nucleic acids. **(A–C)** Sizes of polyplexes loaded with **(A)** EGFP pDNA, **(B)** EGFP mRNA, and **(C)** siRNA against nectin-1. Asterisk represents statistical difference from non-PEGylated polyplexes. **(D–F)** Zeta potentials of polyplexes loaded with **(D)** EGFP pDNA, **(E)** EGFP mRNA, and **(F)** siRNA against nectin-1. **(G–I)** Stability of polyplexes in sodium acetate buffer (25 mM, pH 6.0) over 72 h loaded with **(G)** EGFP pDNA, **(H)** EGFP mRNA, and **(I)** nectin-1 siRNA. **(J–L)** Toxicity of PACE polyplexes compared to Lipofectamine for delivery of **(J)** EGFP pDNA, **(K)** EGFP mRNA, and **(L)** nectin-1 siRNA. Asterisks represent statistical differences between both PACE groups and Lipofectamine. *$p \leq 0.05$, ****$p \leq 0.0001$.

to decrease with the addition of PACE-PEG. The polyplex zeta potentials ranged from −3.1 mV to −22 mV (Fig. 2D–F), and there was no significant difference in zeta potential between non-PEGylated and PEGylated polyplexes, which is likely due to the minimal change in N:P ratio over the PACE-PEG concentrations analyzed (Table S4). PACE-PEG incorporation into polyplexes was confirmed by NMR analysis (Figure S3, Table S3). These results confirm that PACE blended with PACE-PEG forms uniform polyplexes with low polydispersity indices (PDIs) (Figure S4) and without aggregates or sedimentation. At higher concentrations, PACE-PEG can also be used to decrease polyplex size.

3.3. Polyplex stability assessment

PACE polyplexes encapsulating pDNA, mRNA, or siRNA with PACE-PEG content ranging from 0% to 1% were assessed for their stability in sodium acetate buffer (25 mM, pH 6) at 37 °C (Fig. 2G–I). For all nucleic acid types, PACE polyplexes with PACE-PEG incorporation as low as 0.05% were significantly more stable than those without PACE-PEG. Non-PEGylated pDNA (Fig. 2G) and mRNA (Fig. 2H) PACE polyplexes immediately aggregated, whereas addition of 0.25% PACE-PEG provided stability to the polyplexes, allowing them to remain stable over several hours—though they eventually increased in size. In contrast, the addition of 1% PACE-PEG stabilized the PACE polyplexes over 3 days for all nucleic acid types. To assess stability in the presence of negatively charged serum proteins, mRNA polyplexes with and without PACE-PEG were incubated in a solution containing 10% FBS (Figure S5). For non-PEGylated and 0.05% PACE-PEG polyplexes, the addition of serum decreased the vehicle size, but we observed several peaks and the cumulative fit error was high, suggesting that the polyplexes were unstable and too polydisperse to be measured by DLS. Polyplexes with 0.25% PACE-PEG exhibited size variations in 10% FBS, whereas 1% PACE-PEG polyplexes remained stable over 2 days. These results suggest that blending PEG-conjugated PACE with PACE can produce polyplexes with tunable stability properties, and that significant stability can be achieved with PACE-PEG content as low as 0.25%–1% by weight.

3.4. In vitro toxicity studies

PACE and PACE-PEG polyplex toxicity was tested *in vitro* over a range of nucleic acid delivery concentrations. PACE polyplexes were compared to corresponding commercially available Lipofectamine products, prepared according to manufacturer protocols. For pDNA, mRNA, and siRNA polyplexes, cell viability of the non-PEGylated and PEGylated polyplexes was similar, and minimal toxicity was observed—even at higher concentrations (Fig. 2J-L). Cell viability after PACE polyplex treatment was in the range of 70–80% at the highest concentrations of pDNA and mRNA and 90–100% at the highest concentrations of siRNA. By comparison, Lipofectamine showed significant toxicity, with viabilities of 38% (pDNA), 5% (mRNA), and 14% (siRNA) at the

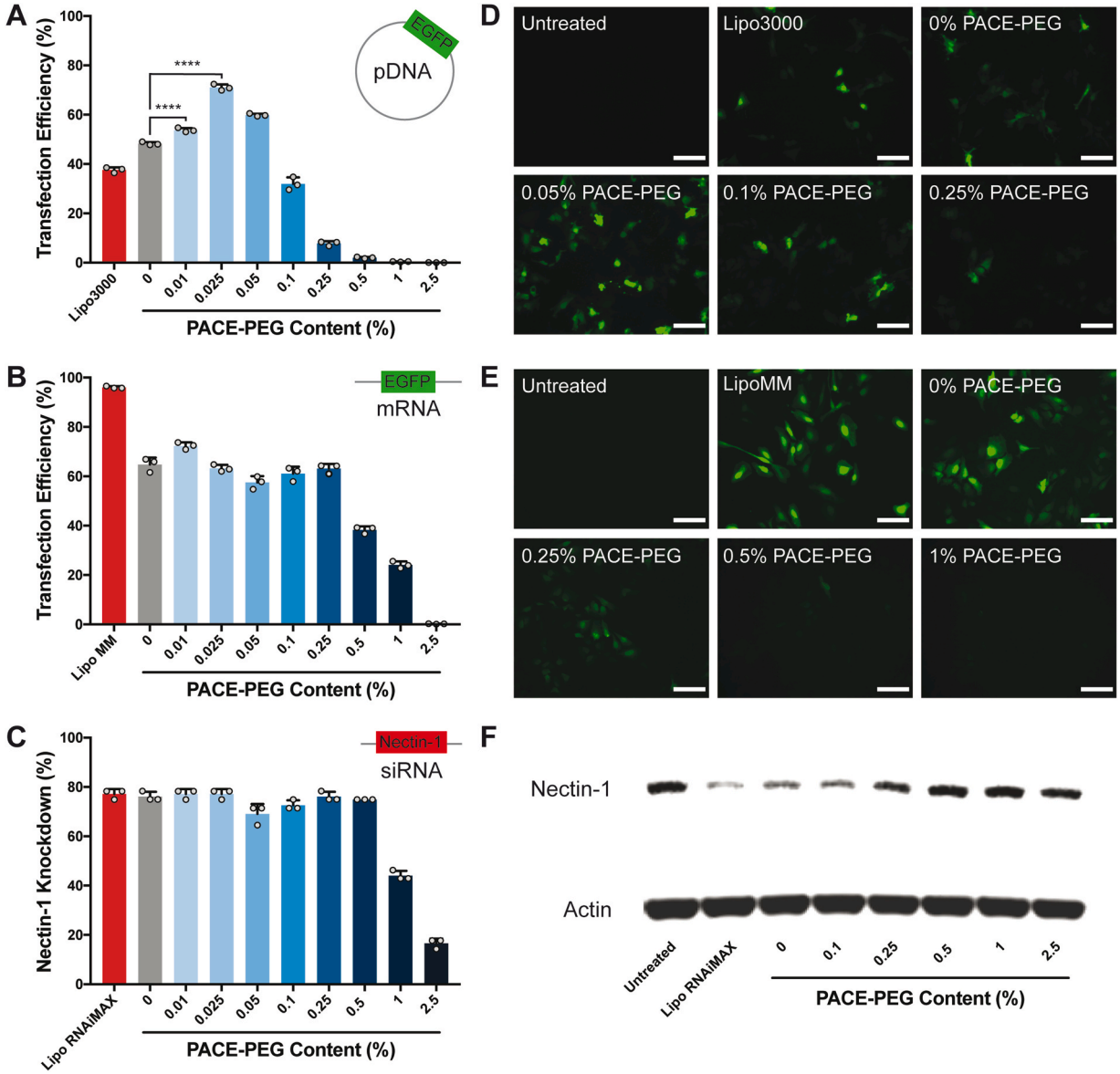

Fig. 3. Low concentrations of PACE-PEG inhibit transfection of PACE polyplexes in a nucleic acid-dependent manner. **(A–C)** Polyplex transfection efficiency measured by flow cytometry for **(A)** pDNA, **(B)** mRNA, and **(C)** knockdown efficiency for siRNA. **(D–E)** EGFP expression in HeLa cells after transfection of EGFP **(D)** pDNA and **(E)** mRNA (scale bar, 100 μm). **(F)** Nectin-1 knockdown by Western blot after delivery of siNectin-1 with PACE-PEG polyplexes. ****$p \leq 0.0001$.

highest measured concentration. Overall, PACE and PACE-PEG-blended polyplexes have a favorable safety profile, likely due to the low charge density of these polymers.

3.5. In vitro transfection of pDNA, mRNA, and siRNA

To assess how PEG content affects PACE polyplex transfection efficiency, we treated HeLa cells with PEGylated PACE polyplexes loaded with pDNA, mRNA, and siRNA and analyzed gene expression as a readout of transfection efficiency by flow cytometry (Fig. 3A–C). For pDNA polyplexes, there was a significant increase in transfection efficiency with low concentrations of PACE-PEG (0.01%, 0.025% 0.05%) compared to the non-PEGylated polyplexes (Fig. 3A). We observed a drop-off in transfection efficiency starting at 0.1% PACE-PEG, and at 1% PACE-PEG no transfection was observed. For mRNA polyplexes, we observed steady transfection up to 0.25% PACE-PEG (Fig. 3B). Starting at 0.5% PACE-PEG, the transfection efficiency dropped until transfection was undetectable at 2.5% PACE-PEG. The pDNA and mRNA transfection results were further confirmed by fluorescence microscopy, which revealed a noticeable decrease in EGFP expression starting at 0.05% PACE-PEG for pDNA and 0.25% PACE-PEG for mRNA (Fig. 3D–E). Small differences observed between the flow cytometry and microscopy trends could be due to batch-to-batch variability in polyplex formulation or a lag between changes in EGFP expression and transfection efficiency. For example, cells might express less EGFP while still maintaining the same percentage of EGFP-positive cells. Lastly, knockdown efficiency with siRNA-loaded polyplexes remained steady from 0% PACE-PEG to 0.5% PACE-PEG and decreased starting at 1% PACE-PEG (Fig. 3C). Since the flow cytometry analysis only captures changes in membrane protein expression, total nectin-1 knockdown was also tested by Western blot (Fig. 3F), which indicated a similar trend. Taken together, these results indicate that blended PACE-PEG polyplexes can effectively transfect a wide variety of nucleic acids as well as—or better than—non-PEGylated polyplexes when the PACE-PEG concentration is below the inhibitory concentration. However, the *in vitro* PACE-PEG inhibitory concentration was very low—as low as 0.1% PACE-PEG by weight in the case of pDNA. We also observed variability in PACE-PEG inhibition between different nucleic acid types, indicating that transfection inhibition by PACE-PEG is nucleic acid-dependent. The inhibitory effect of PEG on nucleic acid transfection may be due to weakened electrostatic interactions between polyplexes and cells [31], which could decrease vehicle uptake [32]. Additionally, improved vehicle stability is hypothesized to prevent polyplexes from aggregating in endosomes and facilitating endosomal escape [20].

3.6. In vivo mRNA delivery

To determine the effect of PACE-PEG content on mRNA transfection *in vivo*, we administered FLuc mRNA using PACE polyplexes with a range of PACE-PEG concentrations by two routes in mice: local intratracheal (IT) delivery to the lung and systemic intravenous (IV) delivery. Twenty-four hours after administration, we observed no transfection in the lung with non-PEGylated (0% PACE-PEG) PACE polyplexes by IT delivery, but luciferase expression increased with the addition of PACE-PEG, peaking at 5% PACE-PEG by weight (Fig. 4A,C). When delivered IV, PACE polyplexes accumulated primarily in the spleen, which is consistent with previous findings [8]. Non-PEGylated polyplexes performed similarly to polyplexes with low levels of PACE-PEG (up to 5%), but transfection was inhibited at higher concentrations (Fig. 4B,D). These results demonstrate that PACE PEGylation can improve

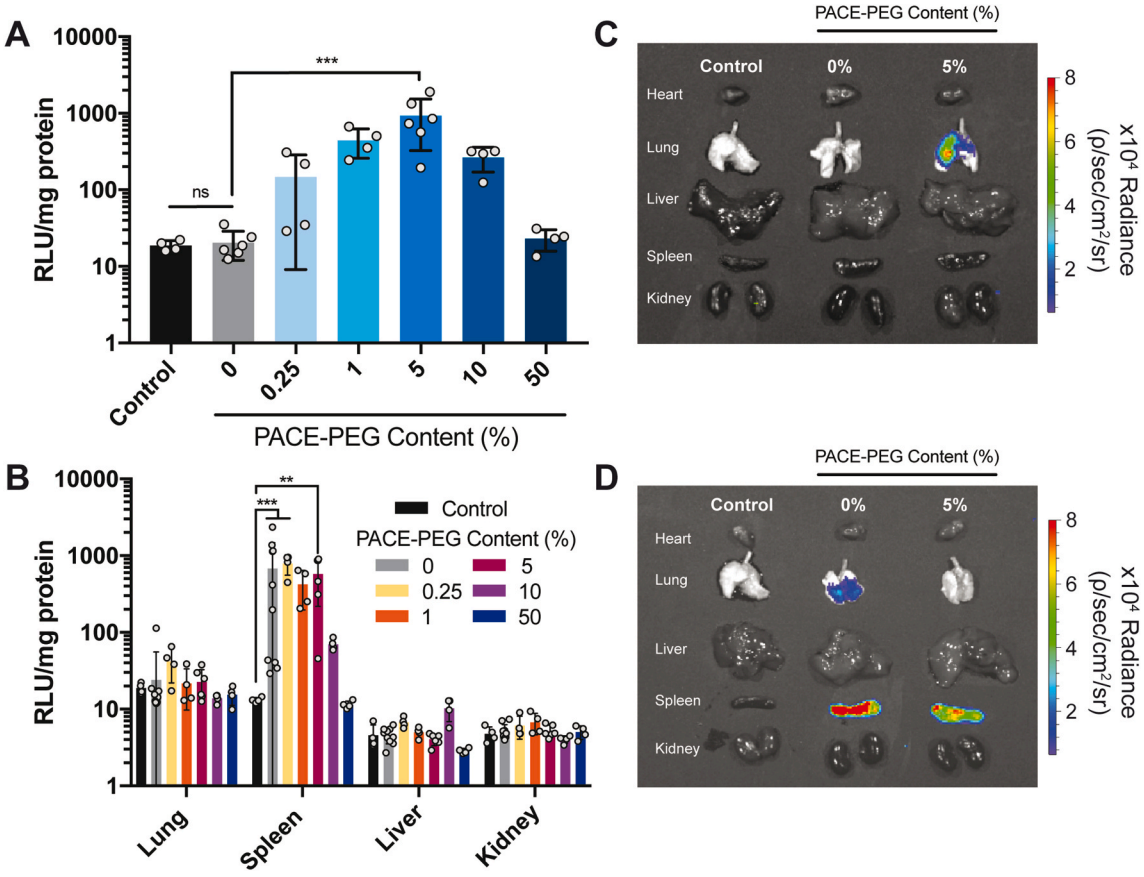

Fig. 4. The effect of PACE-PEG content on *in vivo* mRNA delivery depends on delivery route. FLuc mRNA was delivered using PACE polyplexes blended with PACE-PEG to the lung or systemically by IV delivery. **(A–B)** Luciferase expression in tissue quantified by luminescence assay for **(A)** IT delivery (lungs) and **(B)** IV delivery (lung, spleen, liver, kidney). **(C–D)** Representative IVIS images of luminescence in organs after **(C)** IT and **(D)** IV delivery. $^{**}p \leq 0.01$, $^{***}p \leq 0.001$.

transfection *in vivo*, but the effects vary by delivery route. The fact that higher PEG concentrations are effective—and even beneficial—*in vivo* is likely due to the additional stability PEG provides. Compared to the *in vitro* environment, polyplexes delivered *in vivo* encounter additional physiological barriers with diverse proteins, cell types, and micro-environments, which can affect their transfection efficiency. For example, PEGylation likely improves inhaled delivery to the lung by reducing polyplex aggregation in mucus and facilitating mucus penetration [16]. The observed maximum transfection point at 5% PACE-PEG is the optimal balance of the opposing effects of PEGylation such as improved stability and inhibited transfection. PEGylation is well known to improve carrier circulation times after IV administration [12]. Although we did not observe a beneficial effect on transfection of spleen cells with the addition of low amounts of PEG, we did observe a significant reduction in transfection at higher amounts, demonstrating the potential negative effects of PEG. Reducing polyplex size could improve tissue distribution, since vehicle size has been shown to have a significant effect on NP distribution after IV delivery [33–35]. The PACE formulations developed here successfully deliver mRNA to the lung and spleen, which are organs of interest in a broad range of disease models. For example, gene therapy to the lung has emerged as a promising treatment for cystic fibrosis [36] and a number of respiratory viruses including SARS-CoV-2 [37]. The spleen is critical in mediating the body's immune response, and thus gene therapies delivered to the spleen could be a promising strategy for vaccine delivery [38].

4. Conclusions

In summary, we have demonstrated a simple and robust system of producing PACE polyplexes with tunable PEG content by blending PACE with PACE-PEG in different ratios during formulation. This technique has allowed us to explore the effects of PEG on stability, biocompatibility, and transfection efficiency of PACE polyplexes *in vitro* and *in vivo*. PACE is a highly biocompatible polymer that can effectively deliver a wide variety of nucleic acid cargos, including pDNA, mRNA, and siRNA. We discovered that the addition of low concentrations of PACE-PEG to PACE significantly improved polyplex stability, but also completely inhibited transfection *in vitro*, emphasizing the importance of finding a balance between the advantages and disadvantages of PEGylation—particularly for gene delivery. Furthermore, both the stability benefits and the inhibitory effects of PACE-PEG were influenced by the type of nucleic acid cargo, suggesting that PEGylation for nucleic acid delivery should be optimized to each application. *In vivo*, we discovered that the effects of PACE-PEG varied by delivery route, and low concentrations of PACE-PEG significantly improved inhalation delivery to the lung. We were able use significantly higher concentrations of PACE-PEG compared to *in vitro* experiments before inhibitory effects were seen. These results demonstrate the poor predictive power of *in vitro* experiments on carrier optimization and suggest that the effects of vehicle PEGylation *in vivo* are influenced by additional barriers such as the presence of mucus or serum. Further optimization of this delivery system could be explored through PACE end-group conjugation [8], additional functionalization of the polyplex surface [39], and tuning the PEG MW or polymer to nucleic acid ratio [40]. However, our system is a simple and effective approach at PACE polyplex PEGylation with a wide range of potential applications.

Credit author statement

M.K. Grun: Conceptualization, Methodology, Formal analysis, Investigation, Writing – original draft, Writing – review & editing, Visualization; **A. Suberi**: Investigation; **K. Shin**: Investigation, Writing – review & editing; **T. Lee**: Investigating, Writing – review & editing; **V. Gomerdinger**: Investigation; **Z.M. Moscato**: Investigation; **A.S. Piotrowski-Daspit**: Conceptualization, Resources, Supervision, Writing – original draft, Writing – review & editing; **W.M. Saltzman**: Conceptualization, Supervision, Writing – review & editing, Funding acquisition

Declaration of competing interest

The authors declare that they have no known competing financial interests or personal relationships that could have appeared to influence the work reported in this paper.

Acknowledgements

This research was supported by grants from the National Institutes of Health (NIH; R01 EB00487 and UG3 HL147352). A.S.P. was supported by two NIH National Research Service Awards (NRSAs; a T32 GM86287 training grant and an F32 HL142144 individual postdoctoral fellowship), as well as a postdoctoral research fellowship award (PIOTRO20F0) from the Cystic Fibrosis Foundation (CFF).

Appendix A. Supplementary data

Supplementary data to this article can be found online at https://doi.org/10.1016/j.biomaterials.2021.120780.

Data availability

The raw/processed data required to reproduce these findings cannot be shared at this time as the data also forms part of an ongoing study.

References

[1] J. Chen, K. Wang, J. Wu, H. Tian, X. Chen, Polycations for gene delivery: dilemmas and solutions, Bioconjugate Chem. 30 (2019) 338–349, https://doi.org/10.1021/acs.bioconjchem.8b00688.
[2] A.C. Kauffman, A.S. Piotrowski-Daspit, K.H. Nakazawa, Y. Jiang, A. Datye, W. M. Saltzman, Tunability of biodegradable poly(amine-co-ester) polymers for customized nucleic acid delivery and other biomedical applications, Biomacromolecules 19 (2018) 3861–3873, https://doi.org/10.1021/acs.biomac.8b00997.
[3] E. Fröhlich, The role of surface charge in cellular uptake and cytotoxicity of medical nanoparticles, Int. J. Nanomed. 7 (2012) 5577–5591, https://doi.org/10.2147/IJN.S36111.
[4] A.Yu Kostritskii, D.A. Kondinskaia, A.M. Nesterenko, A.A. Gurtovenko, Adsorption of synthetic cationic polymers on model phospholipid membranes: insight from atomic-scale molecular dynamics simulations, Langmuir 32 (2016) 10402–10414, https://doi.org/10.1021/acs.langmuir.6b02593.
[5] C.-K. Chen, P.-K. Huang, W.-C. Law, C.-H. Chu, N.-T. Chen, L.-W. Lo, Biodegradable polymers for gene-delivery applications, Int. J. Nanomed. 15 (2020) 2131–2150, https://doi.org/10.2147/IJN.S222419.
[6] J. Zhou, J. Liu, C.J. Cheng, T.R. Patel, C.E. Weller, J.M. Piepmeier, Z. Jiang, W. M. Saltzman, Biodegradable poly(amine- co -ester) terpolymers for targeted gene delivery, Nat. Mater. 11 (2012) 82–90, https://doi.org/10.1038/nmat3187.
[7] Y. Liu, Y. Li, D. Keskin, L. Shi, Poly(β-Amino esters): synthesis, formulations, and their biomedical applications, Adv. Healthcare Mater. 8 (2019) 1801359, https://doi.org/10.1002/adhm.201801359.
[8] Y. Jiang, Q. Lu, Y. Wang, E. Xu, A. Ho, P. Singh, Y. Wang, Z. Jiang, F. Yang, G. T. Tietjen, P. Cresswell, W.M. Saltzman, Quantitating endosomal escape of a library of polymers for mRNA delivery, Nano Lett. 20 (2020) 1117–1123, https://doi.org/10.1021/acs.nanolett.9b04426.
[9] A.S. Piotrowski-Daspit, A.C. Kauffman, L.G. Bracaglia, W.M. Saltzman, Polymeric vehicles for nucleic acid delivery, Adv. Drug Deliv. Rev. (2020), https://doi.org/10.1016/j.addr.2020.06.014.
[10] S.-J. Sung, S.H. Min, K.Y. Cho, S. Lee, Y.-J. Min, Y.I. Yeom, J.-K. Park, Effect of polyethylene glycol on gene delivery of polyethylenimine, Biol. Pharm. Bull. 26 (2003) 492–500, https://doi.org/10.1248/bpb.26.492.
[11] H. Petersen, P.M. Fechner, A.L. Martin, K. Kunath, S. Stolnik, C.J. Roberts, D. Fischer, M.C. Davies, T. Kissel, Polyethylenimine-graft-Poly(ethylene glycol) Copolymers: influence of copolymer block structure on DNA complexation and biological activities as gene delivery system, Bioconjugate Chem. 13 (2002) 845–854, https://doi.org/10.1021/bc025529v.
[12] L.G. Bracaglia, A.S. Piotrowski-Daspit, C.-Y. Lin, Z.M. Moscato, Y. Wang, G. T. Tietjen, W.M. Saltzman, High-throughput quantitative microscopy-based half-life measurements of intravenously injected agents, Proc. Natl. Acad. Sci. Unit. States Am. 117 (2020) 3502–3508, https://doi.org/10.1073/pnas.1915450117.
[13] R. Gref, Y. Minamitake, M.T. Peracchia, V. Trubetskoy, V. Torchilin, R. Langer, Biodegradable long-circulating polymeric nanospheres, Science 263 (1994) 1600–1603.

[14] H. Petersen, P.M. Fechner, D. Fischer, T. Kissel, Synthesis, characterization, and biocompatibility of polyethylenimine-graft-poly(ethylene glycol) block copolymers, Macromolecules 35 (2002) 6867–6874, https://doi.org/10.1021/ma012060a.
[15] R. Qi, Y. Gao, Y. Tang, R.-R. He, T.-L. Liu, Y. He, S. Sun, B.-Y. Li, Y.-B. Li, G. Liu, PEG-conjugated PAMAM dendrimers mediate efficient intramuscular gene expression, AAPS J. 11 (2009) 395, https://doi.org/10.1208/s12248-009-9116-1.
[16] Y. Cu, W.M. Saltzman, Controlled surface modification with poly(ethylene)glycol enhances diffusion of PLGA nanoparticles in human cervical mucus, Mol. Pharm. 6 (2008) 173–181.
[17] S.K. Lai, Y.-Y. Wang, K. Hida, R. Cone, J. Hanes, Nanoparticles reveal that human cervicovaginal mucus is riddled with pores larger than viruses, Proc. Natl. Acad. Sci. Unit. States Am. 107 (2010) 598–603.
[18] H. Hatakeyama, H. Akita, H. Harashima, The polyethyleneglycol dilemma: advantage and disadvantage of PEGylation of liposomes for systemic genes and nucleic acids delivery to tumors, Biol. Pharm. Bull. 36 (2013) 892–899, https://doi.org/10.1248/bpb.b13-00059.
[19] C.D. Walkey, J.B. Olsen, H. Guo, A. Emili, W.C.W. Chan, Nanoparticle size and surface chemistry determine serum protein adsorption and macrophage uptake, J. Am. Chem. Soc. 134 (2012) 2139–2147, https://doi.org/10.1021/ja2084338.
[20] S. Mishra, PEGylation significantly affects cellular uptake and intracellular trafficking of non-viral gene delivery particles, Eur. J. Cell Biol. 83 (2004) 97–111.
[21] T. Ishida, R. Maeda, M. Ichihara, K. Irimura, H. Kiwada, Accelerated clearance of PEGylated liposomes in rats after repeated injections, J. Contr. Release 88 (2003) 35–42, https://doi.org/10.1016/S0168-3659(02)00462-5.
[22] M. Ichihara, T. Shimizu, A. Imoto, Y. Hashiguchi, Y. Uehara, T. Ishida, H. Kiwada, Anti-PEG IgM response against PEGylated liposomes in mice and rats, Pharmaceutics 3 (2011) 1–11, https://doi.org/10.3390/pharmaceutics3010001.
[23] S. Mao, M. Neu, O. Germershaus, O. Merkel, J. Sitterberg, U. Bakowsky, T. Kissel, Influence of polyethylene glycol chain length on the physicochemical and biological properties of poly(ethylene imine)-graft-Poly(ethylene glycol) block copolymer/SiRNA polyplexes, Bioconjugate Chem. 17 (2006) 1209–1218, https://doi.org/10.1021/bc060129j.
[24] R.E.B. Fitzsimmons, H. Uludağ, Specific effects of PEGylation on gene delivery efficacy of polyethylenimine: interplay between PEG substitution and N/P ratio, Acta Biomater. 8 (2012) 3941–3955, https://doi.org/10.1016/j.actbio.2012.07.015.
[25] A. Malek, F. Czubayko, A. Aigner, PEG grafting of polyethylenimine (PEI) exerts different effects on DNA transfection and siRNA-induced gene targeting efficacy, J. Drug Target. 16 (2008) 124–139, https://doi.org/10.1080/10611860701849058.
[26] X. Zhang, S.-R. Pan, H.-M. Hu, G.-F. Wu, M. Feng, W. Zhang, X. Luo, Poly(ethylene glycol)-block-polyethylenimine copolymers as carriers for gene delivery: effects of PEG molecular weight and PEGylation degree, J. Biomed. Mater. Res. 84A (2008) 795–804, https://doi.org/10.1002/jbm.a.31343.
[27] Z. Zhong, J. Feijen, M.C. Lok, W.E. Hennink, L.V. Christensen, J.W. Yockman, Y.-H. Kim, S.W. Kim, Low molecular weight linear polyethylenimine-b-poly(ethylene glycol)-b-polyethylenimine triblock Copolymers: synthesis, characterization, and in vitro gene transfer properties, Biomacromolecules 6 (2005) 3440–3448, https://doi.org/10.1021/bm050505n.
[28] P. Mastorakos, C. Zhang, S. Berry, Y. Oh, S. Lee, C.G. Eberhart, G.F. Woodworth, J. S. Suk, J. Hanes, Highly PEGylated DNA nanoparticles provide uniform and widespread gene transfer in the brain, Adv. Healthcare Mater. 4 (2015) 1023–1033, https://doi.org/10.1002/adhm.201400800.
[29] J.-M. Williford, M.M. Archang, I. Minn, Y. Ren, M. Wo, J. Vandermark, P.B. Fisher, M.G. Pomper, H.-Q. Mao, Critical length of PEG grafts on lPEI/DNA nanoparticles for efficient in vivo delivery, ACS Biomater. Sci. Eng. 2 (2016) 567–578, https://doi.org/10.1021/acsbiomaterials.5b00551.
[30] Y. Fang, J. Xue, S. Gao, A. Lu, D. Yang, H. Jiang, Y. He, K. Shi, Cleavable PEGylation: a strategy for overcoming the “PEG dilemma” in efficient drug delivery, Drug Deliv. 24 (2017) 22–32, https://doi.org/10.1080/10717544.2017.1388451.
[31] R.N. Majzoub, C.-L. Chan, K.K. Ewert, B.F.B. Silva, K.S. Liang, E.L. Jacovetty, B. Carragher, C.S. Potter, C.R. Safinya, Uptake and transfection efficiency of PEGylated cationic liposome–DNA complexes with and without RGD-tagging, Biomaterials 35 (2014) 4996–5005, https://doi.org/10.1016/j.biomaterials.2014.03.007.
[32] P.G. Millili, J.A. Selekman, K.M. Blocker, D.A. Johnson, U.P. Naik, M.O. Sullivan, Structural and functional consequences of poly(ethylene glycol) inclusion on DNA condensation for gene delivery, Microsc. Res. Tech. 73 (2010) 866–877, https://doi.org/10.1002/jemt.20839.
[33] W.-Y. Liao, H.-J. Li, M.-Y. Chang, A.C.L. Tang, A.S. Hoffman, P.C.H. Hsieh, Comprehensive characterizations of nanoparticle biodistribution following systemic injection in mice, Nanoscale 5 (2013) 11079–11086, https://doi.org/10.1039/C3NR03954D.
[34] W.H. De Jong, W.I. Hagens, P. Krystek, M.C. Burger, A.J.A.M. Sips, R.E. Geertsma, Particle size-dependent organ distribution of gold nanoparticles after intravenous administration, Biomaterials 29 (2008) 1912–1919, https://doi.org/10.1016/j.biomaterials.2007.12.037.
[35] H.K. Mandl, E. Quijano, H.W. Suh, E. Sparago, S. Oeck, M. Grun, P.M. Glazer, W. M. Saltzman, Optimizing biodegradable nanoparticle size for tissue-specific delivery, J. Contr. Release 314 (2019) 92–101, https://doi.org/10.1016/j.jconrel.2019.09.020.
[36] U. Griesenbach, E.W.F.W. Alton, Moving forward: cystic fibrosis gene therapy, Hum. Mol. Genet. 22 (2013) R52–R58, https://doi.org/10.1093/hmg/ddt372.
[37] L. Du, G. Zhao, Y. Lin, H. Sui, C. Chan, S. Ma, Y. He, S. Jiang, C. Wu, K.-Y. Yuen, D.-Y. Jin, Y. Zhou, B.-J. Zheng, Intranasal vaccination of recombinant adeno-associated virus encoding receptor-binding domain of severe acute respiratory syndrome coronavirus (SARS-CoV) spike protein induces strong mucosal immune responses and provides long-term protection against SARS-CoV infection, J. Immunol. 180 (2008) 948–956, https://doi.org/10.4049/jimmunol.180.2.948.
[38] A.B. Jindal, Nanocarriers for spleen targeting: anatomo-physiological considerations, formulation strategies and therapeutic potential, Drug Deliv. and Transl. Res. 6 (2016) 473–485, https://doi.org/10.1007/s13346-016-0304-0.
[39] G.T. Tietjen, S.A. Hosgood, J. DiRito, J. Cui, D. Deep, E. Song, J.R. Kraehling, A. S. Piotrowski-Daspit, N.C. Kirkiles-Smith, R. Al-Lamki, S. Thiru, J.A. Bradley, K. Saeb-Parsy, J.R. Bradley, M.L. Nicholson, W.M. Saltzman, J.S. Pober, Nanoparticle targeting to the endothelium during normothermic machine perfusion of human kidneys, Sci. Transl. Med. 9 (2017), https://doi.org/10.1126/scitranslmed.aam6764.
[40] Y. Jiang, A. Gaudin, J. Zhang, T. Agarwal, E. Song, A.C. Kauffman, G.T. Tietjen, Y. Wang, Z. Jiang, C.J. Cheng, W.M. Saltzman, A “top-down” approach to actuate poly(amine-co-ester) terpolymers for potent and safe mRNA delivery, Biomaterials 176 (2018) 122–130, https://doi.org/10.1016/j.biomaterials.2018.05.043.